

# **Theoretical study of the passage of chloride ions through bacterial ClC chloride channels**

Gennady V. Miloshevsky and Peter C. Jordan

Department of Chemistry, Brandeis University, Waltham, Massachusetts  
(Sponsor: Criss Hartzell)

## **Abstract**

X-ray structures [1,2] permit theoretical study of Cl<sup>-</sup> permeation along the curvilinear pores of the bacterial ClC Cl<sup>-</sup> channels. Metropolis Monte Carlo (MMC) simulations are used to determine the coordinates of the lowest energy pathway; the helices and amino acids that line the conduction path and that coordinate the translocating anion. We find that all four crystallographic structures of the bacterial ClC Cl<sup>-</sup> channels correspond to closed states. E148 and S107 side chains form steric barriers on both sides of the crystal binding site in the StClC WT and EcClC WT structures; both the EcClC E148A and EcClC E148Q mutants are blocked at S107 site. We examine the effect that the charge state of E111, E148 and R147 amino acids has on anion permeation by calculating electrostatic potential energy profiles. These suggest a reasonable anion conduction mechanism: neutralize E148, then trap the anion at the E148 locus, and finally either deprotonate E148 or bring a second Cl<sup>-</sup> into the pore. We note also that the charge state of E111 may electrostatically control anion conductance within the cytoplasmic pore [3]. Finally, we analyze a possible pathway at interface between subunits A and B for moving a 9-AC inhibitor towards its recently discovered binding pocket [4].

## Introduction

The X-ray structures of the bacterial ClC Cl channels [1,2] confirm that these channels are double-barrel dimers [5] formed of identical subunits (**Figure 1**) that contact each other at a broad interface and span a membrane slab with antiparallel orientations. In each subunit almost all helices are tilted; many do not span the bilayer. Each subunit has its own independent Cl<sup>-</sup> conducting pore. The most recent X-ray study [2] begins to provide detailed insight into the coupling between conduction and gating. However, what remains unclear are the atomic particulars of anion translocation in the open channel, the specific interactions that may permit several chlorides to occupy the pathways simultaneously [2], the precise role of the anion-coordinating amino acids and the details of their interaction with the anions. Theoretical studies of the bacterial ClC channels might help in understanding ClC channel function.

We provide a detailed description of the coordination of the Cl<sup>-</sup> ions during their translocation through the pore. To get an intuitive feeling, we examine the effect that E111, E148 and R147 amino acids have on anion coordination by calculating electrostatic potential profiles. These clearly demonstrate electrostatic barriers and wells that Cl<sup>-</sup> experiences during translocation. The potential wells reveal positions (binding sites) on the permeation pathway that may be preferentially occupied by Cl<sup>-</sup>. Also, using the four crystal structures we identified a possible route along the interface between subunits A and B for movement of a 9-AC inhibitor towards its partially hydrophobic binding pocket.

## Computational Model

MMC simulations are performed using our *MCICP* (*Monte Carlo Ion Channel Proteins*) code with the following assumptions (**Figure 1**):

- Two subunits of the ClC Cl<sup>-</sup> protein are immersed in a low dielectric ( $\epsilon = 1$ ) membrane slab. The protein mouths of subunit A were filled by explicit water molecules (~1,500-2,000) located in a cylinder of 25 Å radius, centered on the central binding site of subunit A. Bulk water regions are treated as continua with  $\epsilon = 80$ . The reaction field is treated by the method of images; van der Waals and electrostatic interactions are computed with no cutoff.
- We use partial charges and van der Waals parameters of the CHARMM22 all-hydrogen force field. The four crystallographic X-ray structures of the bacterial ClC Cl<sup>-</sup> channels [1,2] (StClC (pdb entry 1KPL) and three EcClC (pdb entries 1OTS, 1OTT (E148A mutant) and 1OTU (E148Q mutant)) channels) were used in the MMC simulations. During simulations of chloride translocation, the ClC Cl<sup>-</sup> protein is treated as a rigid body.
- A *KMCRPF* technique [6] was used to determine the coordinating residues and lowest energy paths, delineating putative pathways through the curved ClC pores. A preferential sampling technique was incorporated to move the water molecules near the anion more frequently than those further away.

## Calculating the Anion Interaction Energy

Cl<sup>-</sup> conduction pathways are characterized by curvilinear pores with wide vestibules on both extracellular and cytoplasmic sides and narrow Cl<sup>-</sup> selective regions in mid-channel. Determination of the ion-protein interaction energy along these curved paths is not straightforward, as the coordinates of the lowest energy path are unknown.

A kinetic MC technique [6] was used to determine reaction pathways (*Kinetic Monte Carlo Reaction Path Following (KMCRPF)*). The MMC method permits moves to higher energy states with Boltzmann probability. The smaller the energy difference the greater the probability of an acceptable uphill move. Thus the ion's Z coordinate (coordinate along the curved pore) was only allowed to increase. Ionic X & Y coordinates were freely variable. The reaction coordinate (Z coordinate) evolves slowly relative to the other degrees of freedom. As the ion approaches a saddle point with rapidly increasing energy, only small changes in Z are likely to be accepted. This describes a major aspect of the motion along the reaction pathway. For each new configuration several MC trials with the new Z coordinate fixed were followed to relax the ion. The remaining degrees of freedom then relax fully in response to movement along the reaction coordinate, an especially important feature as the ion evolves downhill, since any new configuration with lower energy is always accepted. The *KMCRPF* technique allows the ion to overcome steep electrostatic and steric barriers in following the lowest energy path.

## Conduction Pathway and Chloride-Coordinating Amino Acids

A Cl<sup>-</sup> ion was placed at the central crystallographic site in subunit A and MMC simulations were carried out using the *KMCRPF* technique. The ionic pathway was followed by moving away from the binding site and towards the cytoplasm and periplasm, thus determining the lowest energy pathways and the corresponding anion interaction energy profiles.

**Figure 2** illustrates the anion conduction pathway (green curve) through pore A in the StClC WT structure. The pore length is about 16 Å. Pore lining  $\alpha$ -helices and residues are shown. In the cytoplasmic region the pore is lined by helices R and D. At the extracellular entrance and in mid-membrane the ion pathway is coordinated by helices F and N. The water molecules are illustrated in the cavities approaching the pore from the cytoplasmic ( $\sim -6$  Å) and extracellular ( $\sim 10$  Å) sides. In the cytoplasm the pore entrance is formed by I448, S107, P110, F348 and Y445. In all four crystal structures (StClC, EcClC and its two mutants) the side chain of S107 sterically restricts ion entrance into the pore from the cytoplasmic region. At the central binding site the anion (green sphere) is coordinated by backbone HNs of I356 and F357 (helix N) and by hydroxyl HOs of Y445 and S107. In the periplasm the pore entrance is formed by G146, R147, E148, F190 and A358. The side chain of R147 is easily accessible to water molecules. Then the E148 side chain, which forms bonds with numerous protein hydrogens, blocks the pathway in the wild-type (WT) StClC and EcClC crystal structures.

**Figure 3** illustrates residues on the anion's pathway in the cytoplasmic part of pore A in StClC. At  $\sim -6$  Å (the internal binding site [2]) the anion faces the intracellular water molecules. Side chains of P110, I448 and F348 (Fig. 3a) coordinate the anion's entrance into the pore. On the other side of the pore (Fig. 3a) the anion is coordinated by backbone HNs from the end of helix D (G108 and S107). In the StClC and EcClC WT crystal structures and both EcClC mutants S107 sterically restricts ion entrance into the central binding site (Fig. 3b). The steric block is due to OG and CB of S107 and OH and CE2 of Y445. The constricted pore radius at this site ( $-2.7$  Å) is about 1 Å. Note that the residues adjacent to S107 are glycines; the side chains of S107 and Y445 may both be easily mobile to open the pore. At the central binding site (Fig. 3c) the anion is coordinated by backbone HNs of I356 and F357 and hydroxyl HOs of Y445 and S107 [1]. Backbone HNs of I109 and G149 also contribute to the anion coordination. The anion fits perfectly in the central binding site (pore radius  $\sim 1.8$  Å).

**Figure 4** illustrates residues on the pathway in the extracellular part of pore A in StClC. At the entrance ( $\sim 10$  Å) the anion is coordinated by side chain of R147 and by backbone HNs from G315, G316 and F317 (Fig. 4a). This site is accessible to water molecules and the anion also interacts with three or four waters (see Fig. 2). The E148 oxygens block the pathway forming the hydrogen bonds with HNs from E148, R147, G149, A358 and HAs from G146 and G355 (Fig. 4b). The constricted pore radius at this site ( $\sim 4.8$  Å) is about 0.5 Å.

## Anion electrostatic potential energy profiles

As the pore is sterically constricted, the total non-bonded interaction energy has no meaning. However, the electrostatic potential energy profile along the path may provide the clues on the energy barriers and wells in the open pore. Our rationale is that the blocking residues must slightly rearrange themselves [2] in order for the pore to open and the anion to move unimpeded. These local processes most likely do not require global structural alterations.

**Figure 5** illustrates electrostatic potential energy profiles along the pathway in pore A of the EcClC WT structure. In the cytoplasmic and extracellular mouths the anion is solvated by the water molecules. In the pore region there are large electrostatic barriers at E148 and S107 sites (see Fig. 2). These barriers are somewhat overestimated as the anion passes very close to the glutamate and serine oxygens (the pore is constricted). Here we focus on the charge states of E111, E148 and R147. The barrier at  $Z \sim 4 \text{ \AA}$  is due to the charge of E148 (black curve). Mutating E148A [2] or neutralizing E148 by lowering pH [7] creates a deep electrostatic trap. The barrier near  $4 \text{ \AA}$  disappears (red curve). Mutating S107 to glycine also affects the barrier at the S107 site. For the E148A or E148Q mutants the behavior of the electrical potential energy profile is very close to that of neutralized E148 with R147 in its native state. The energy minimum at  $Z \sim 4 \text{ \AA}$  is then located precisely at the position previously occupied by the oxygens from E148 (the external binding site [2]). The barrier near  $4 \text{ \AA}$  shifts toward  $10 \text{ \AA}$  if the charge conserved R147 is neutralized by proton transfer to E148 (green curve). Neutralizing E111 effects energetics in the cytoplasmic mouth [3] (blue curve). Energy wells appear at  $\sim -6 \text{ \AA}$  (the internal binding site [2]) and at  $\sim -11 \text{ \AA}$ .

## The 9-anthracene carboxylic acid inhibitor binding center

Recently the S537 residue of ClC-1 between helices O and P (corresponding to V402 in StClC and I402 in EcClC) was identified as an inhibitor binding center for 9-anthracene carboxylic acid (9-AC) [4]. It was concluded that a partially hydrophobic inhibitor binding pocket, only accessible from the cytoplasm, is located near the central Cl<sup>-</sup> binding site. To study this putative inhibitor binding pocket using the StClC and EcClC crystal structures we constructed a sphere with radius 15 Å centered on the  $\alpha$ -carbon (CA) of V402 (StClC) or I402 (EcClC) and tried to insert an anionic hard sphere of radius 1.7 Å (the minimum “hard core” half thickness of 9-AC) anywhere inside this region; protein vdW radii were also reduced (by a factor of 0.8) to mimic hard spheres. Within this 15 Å sphere, we made 10<sup>8</sup> random trials to identify a possible route for 9-AC towards the putative inhibitor binding pocket.

**Figure 6** illustrates the sites (black spheres with numbers) where it is possible to insert a hard sphere of radius 1.7 Å in the EcClC E148Q mutant. The inhibitor site is denoted 9-AC. In all four crystal structures there is a large cleft at the interface between subunits A and B (sites 1-4), which is readily accessible from the cytoplasmic side for a bulky group like 9-AC (Fig. 6a). Here the interface is formed by residues G441, K442, Q207 and helices J (Q270), R (P443, S446, A447), H (E202) from subunit A and by residues R28, D29 and helices A (L25, L26), I (I215), H (I201) from subunit B. The side chain of R403 is in contact with water molecules. However, in all four crystal structures there is no direct route from this region along the side chain of R403 to V402 (the 9-AC inhibitor binding pocket).

A putative pathway was found in the EcClC E148Q structure close to a two-fold axis (sites 5-7). Sites 5-7 are within 4-5 Å of each other. The path is formed by helices H (I201, E202), P (P405, L406, I409), Q (I426, G429, L430) from subunit A and by helices H (I201), I(215, K216, F219) from subunit B (Fig. 6b). Most of the coordinating residues are hydrophobic. The side chains of the charged residues point away from the path and coordination is due to the non-polar backbone atoms from those residues. Sites 8, 9 and 9-AC are located within an inhibitor binding pocket discovered in [4]. Here the coordinating helices are P (A404, P405, L406, T407, G408, I409, V412), O (I391, A392, G393, M394, G395, A396, L398, A399, I402) and Q (M425, G429) from subunit A. Sites 3-9 are clustered in a wide region that is accessible from the cytoplasm (see the view from the cytoplasm in Fig. 6b).

We examined the four crystal structures of the bacterial ClC channel to identify a possible pathway towards the putative inhibitor binding pocket. The conformational states of these structures differ, but ensemble they reveal a possible way for 9-AC to access the binding site. In WT StClC only site 8 can accommodate an anionic hard sphere of radius 1.7 Å; there is not enough room at sites 5-7, 9 or 9-AC. Sites 8 and 9-AC of WT EcClC are big enough, but sites 5-7 and 9 are too small. In EcClC E148A sites 8 and 10 (the black square in Fig. 6) are acceptable. Site 10 is located between the 9-AC site and the central anion binding site. The distance from site 10 to the anion is about 5 Å. Finally, in EcClC E148Q the sites illustrated in Fig. 6 are all large enough. Thus, comprehensive analysis of the four crystal structures suggests that 9-AC can reach its binding site along the interface between subunits A and B and may then affect the anion pathway near the central Cl<sup>-</sup> binding site.

## Conclusions

- The X-ray structures of the bacterial ClC Cl<sup>-</sup> channels correspond to closed states. In addition to E148 the side chain of S107 sterically impedes ionic passage from the binding site into the cytoplasm in all four structures. In both the EcClC E148A and EcClC E148Q mutants there is a small steric barrier near E148. It suggests that the anion fits snugly the whole length of the pore and that protein flexibility is crucial in treating anion permeation.
- When the E148 is mutated or neutralized, it creates an electrostatic trap, binding the anion near mid-membrane. To escape the trap, the neutralized E148 could be deprotonated and its side chain dislodged (required to relieve the steric barrier) and replaced by another incoming Cl<sup>-</sup>, in which case there is an electrical gradient promoting ion flow. Side chain displacement may arise by competition for the binding site between the oxygens of neutralized E148 and the anion moving down the electrostatic energy gradient. The highly conserved E111 might electrostatically control anion conductance and occupancy of the internal binding site in the cytoplasmic pore [3].
- Exploring the four crystal structures a possible pathway leading to a partially hydrophobic pocket for inhibitors [4] was identified at the interface between subunits A and B. The coordination on this pathway is due to the hydrophobic side chains from helices H, P, Q (subunit A) and H, I (subunit B). The flexibility of these side chains may allow a room for a large group like 9-AC to reach its putative binding pocket. This pocket may be also accessible from the central Cl<sup>-</sup> binding site. However, in the crystal structures the pore is highly constricted between the S107 and Y445 residues (Fig. 3b).

## Acknowledgements

Work supported by an NIH grant, GM-28643.


## References

1. R. Dutzler et al., *Nature*. **415**:287-294 (2002)
2. R. Dutzler et al., *Science*. **300**:108-112 (2003)
3. M.-F. Chen & T.-Y. Chen, *J. Gen. Phys.* **122**:133-145 (2003)
4. R. Estévez et al., *Neuron*. **38**:47-59 (2003)
5. C. Miller & M.M. White, *Proc. Natl. Acad. Sci. USA* **81**:2772-2775 (1984)
6. G.V. Miloshevsky & P.C. Jordan, *Biophys. J.* **84**:412a (2003)
7. A. Accardi & C. Miller, 57<sup>th</sup> SGP Meeting (2003), MBL Woods Hole, MA. Poster 37.

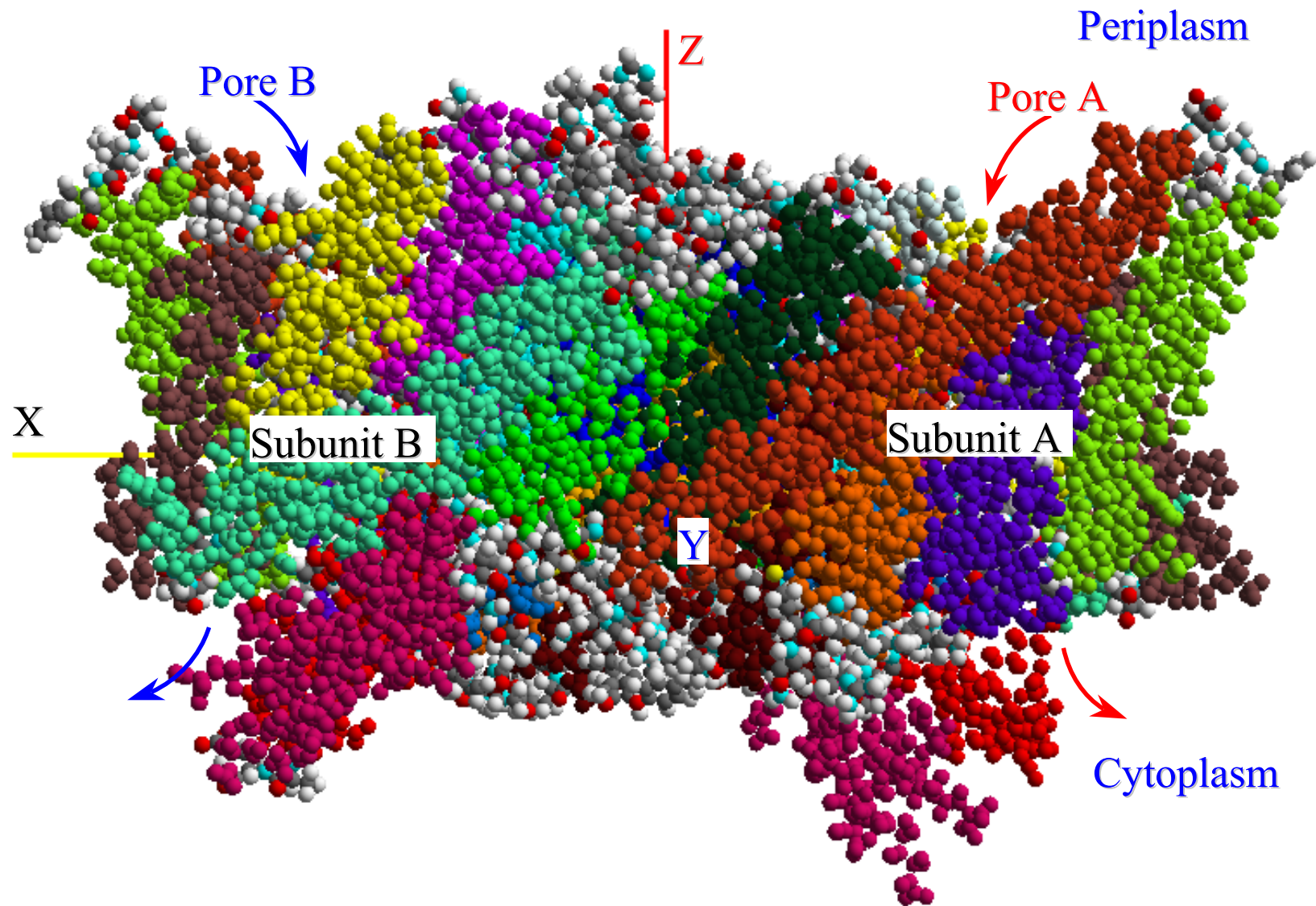


**Figure 1.** Molecular representation of the ClC Cl<sup>-</sup> channel. View from within the membrane with the cytoplasm below. Both StClC subunits are shown. The transmembrane  $\alpha$ -helices are color-coded. The ion pathways are shown as curved arrows.

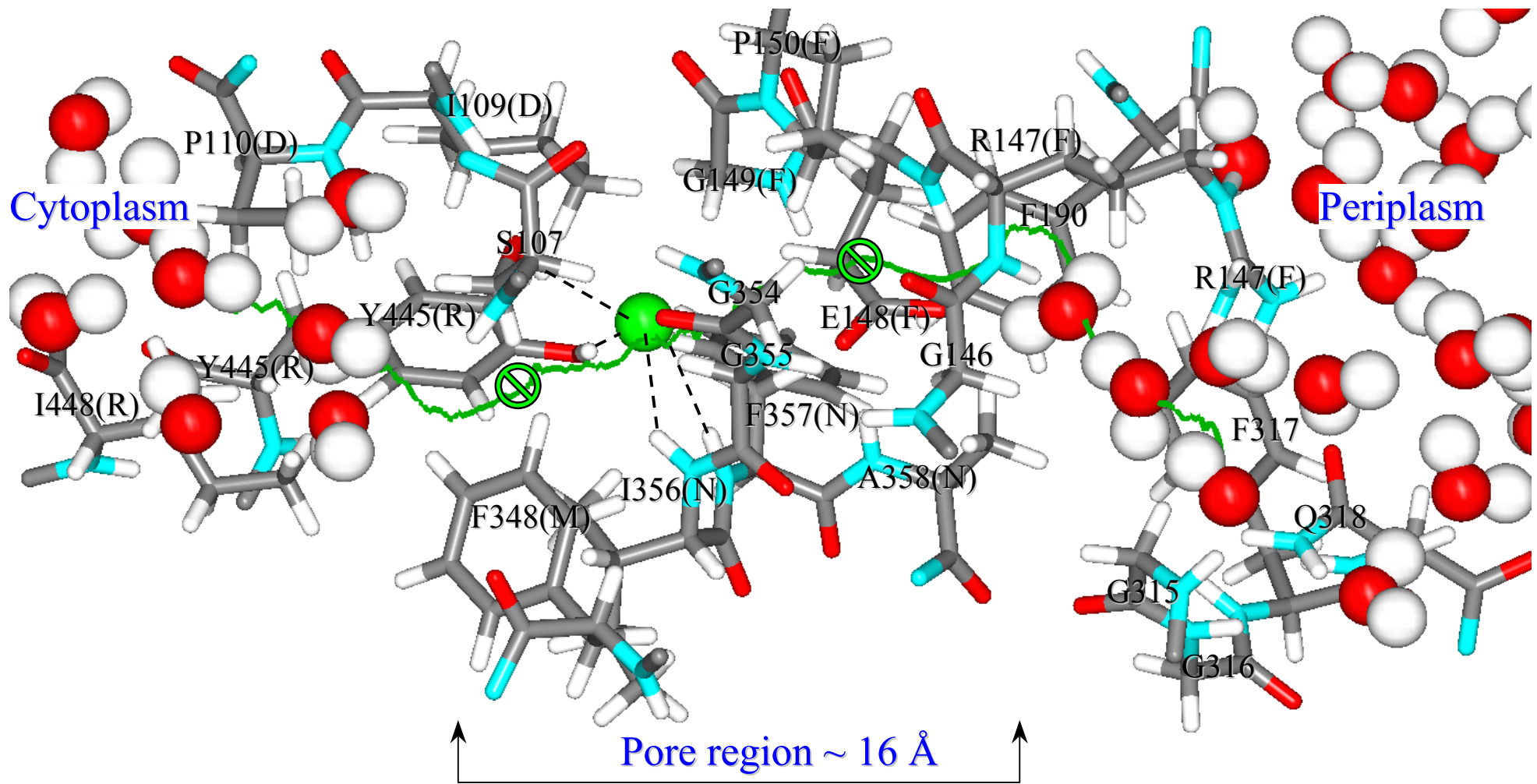


**Figure 2.** Anion pathway along pore A in StClC. The Cl<sup>-</sup> trajectory is represented by the green curve. The anion in the central binding site is illustrated as a green sphere. The symbol  indicates sites where the pore is blocked. Important helices and residues lining the pore are labeled. Water molecules in the ClC protein mouths are illustrated.

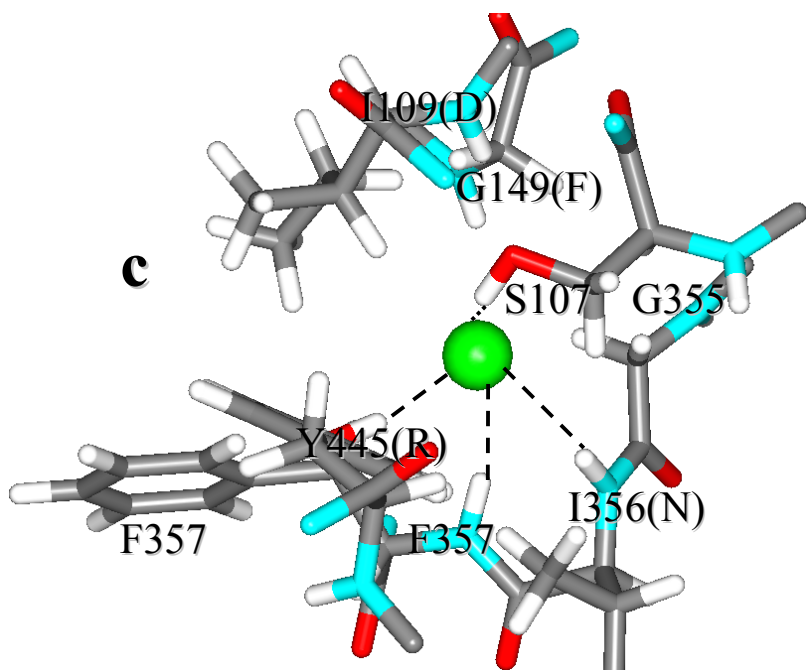
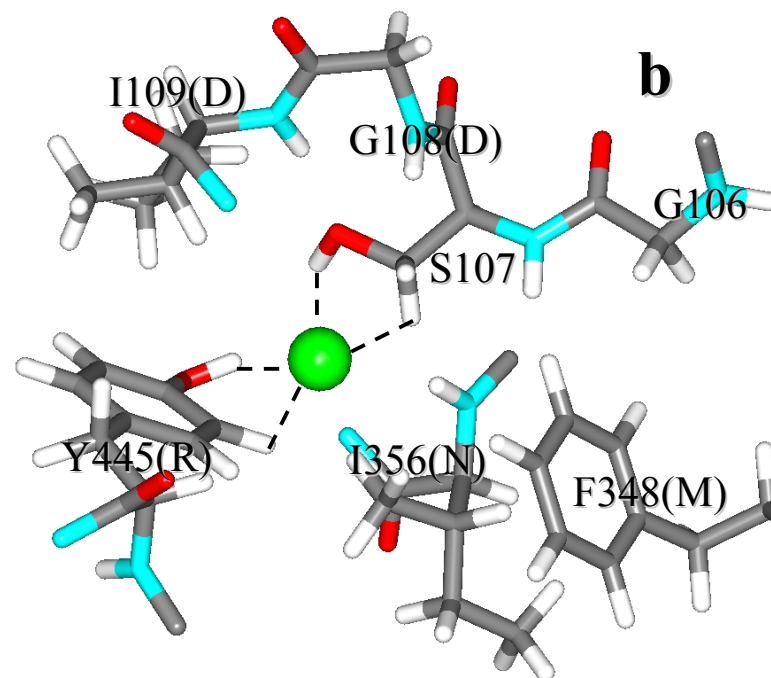
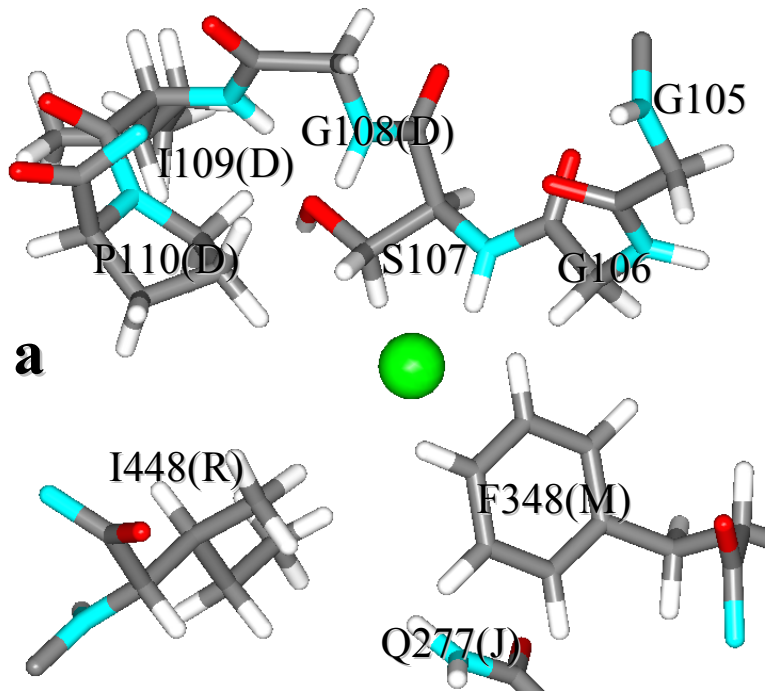


**Figure 3.** Residues defining the  $\text{Cl}^-$  ion conduction pore A pathway in the cytoplasmic region of StClC. The view is along the pore from the cytoplasmic side.  $\text{Cl}^-$  is represented as a green sphere. **a:**  $\text{Cl}^-$  located at  $Z = -6 \text{ \AA}$  (the internal binding site). **b:**  $\text{Cl}^-$  located at  $Z = -2.7 \text{ \AA}$  (steric barrier due to S107). **c:**  $\text{Cl}^-$  located at its central binding site,  $Z = 0 \text{ \AA}$ .

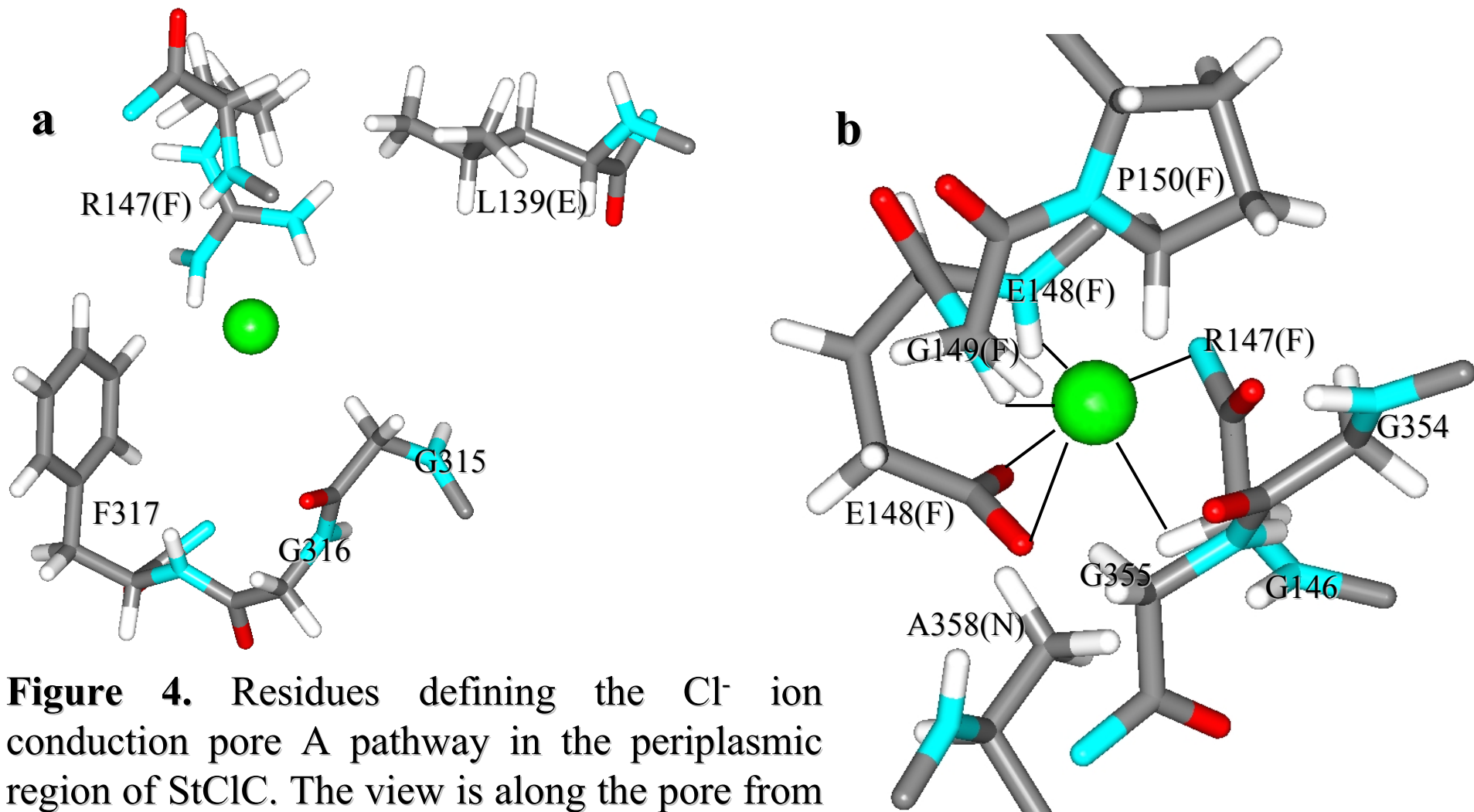


**Figure 4.** Residues defining the  $\text{Cl}^-$  ion conduction pore A pathway in the periplasmic region of StClC. The view is along the pore from the cytoplasmic side.  $\text{Cl}^-$  is represented as a green sphere. **a:**  $\text{Cl}^-$  located at  $Z = 10 \text{ \AA}$  (the entrance from the periplasm). **b:**  $\text{Cl}^-$  located at  $Z = 4.8 \text{ \AA}$ . The E148 side chain blocks the pore.

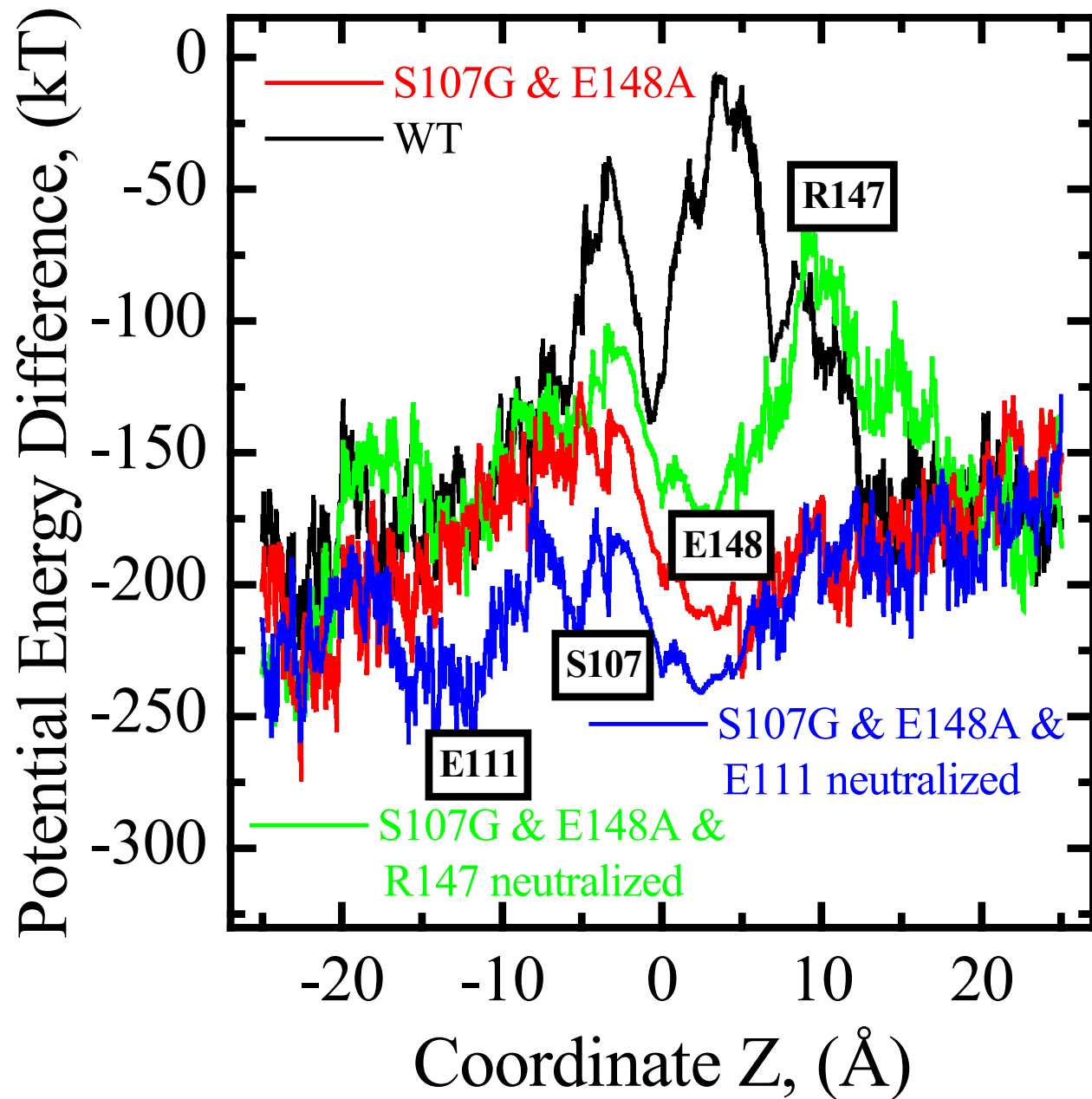


**Figure 5.** Electrostatic potential energy profiles as functions of the Z-coordinate along the pore A pathway. The locations of E111, S107, E148 and R147 are labeled. The black curve is for the native state of the EcClC WT channel (both E148 and R147 are charged). The red curve illustrates the effect of mutating E148A or neutralizing E148 by pH decrease. Here S107 is mutated to glycine. The green curve describes the case where R147 is also neutralized by proton transfer to E148. Finally, the blue curve shows the effect of also neutralizing E111 in the cytoplasmic mouth.

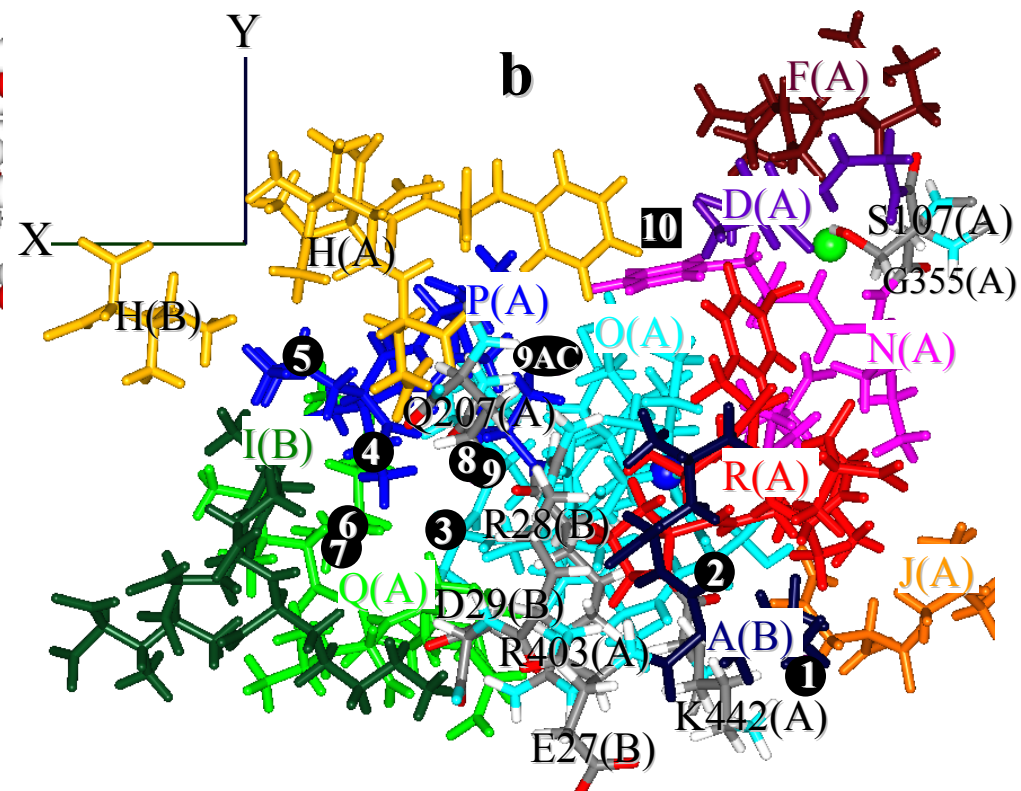
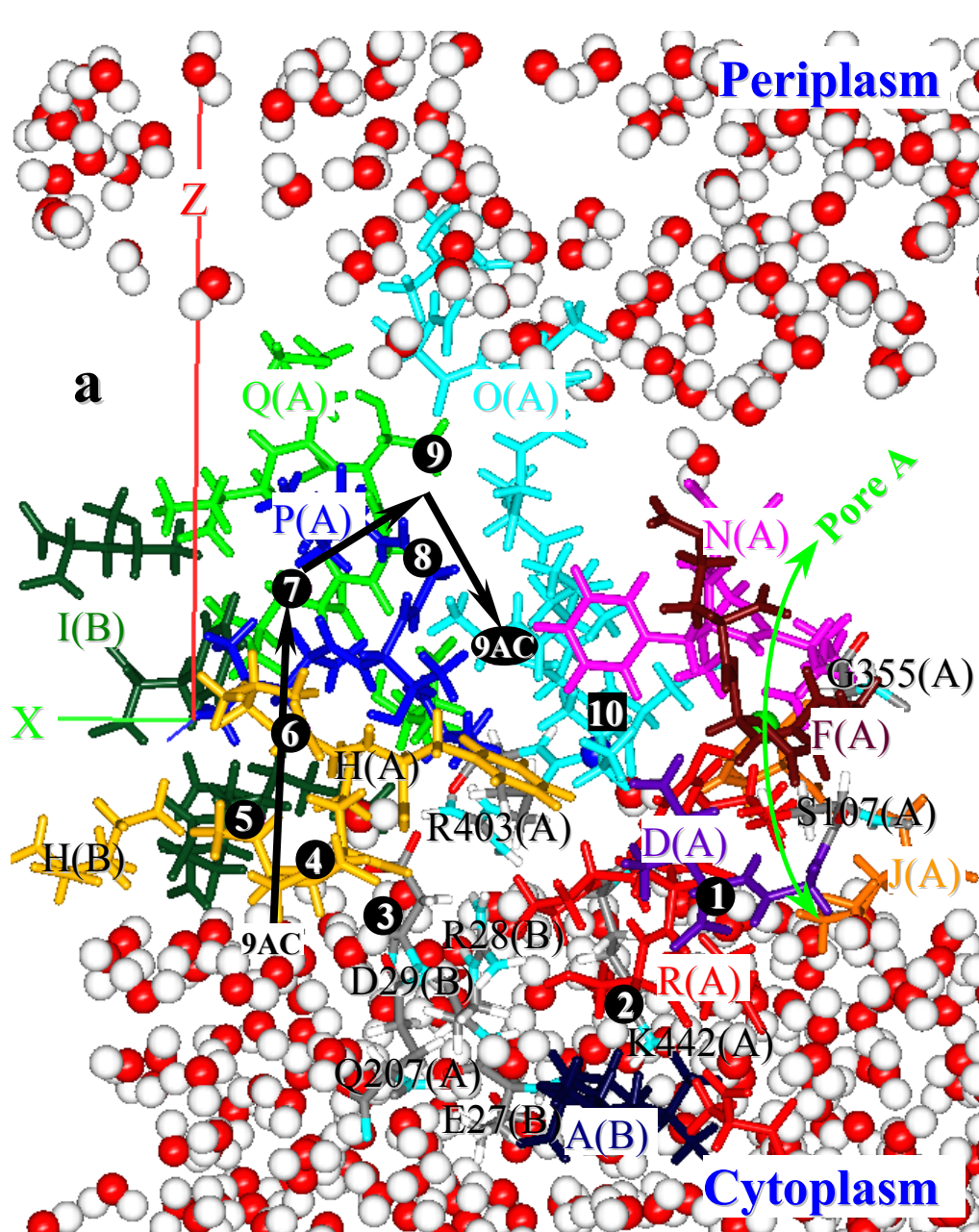


**Figure 6.** The putative route (black arrows) towards the inhibitor binding pocket in the EcClC E148Q mutant. Sites defining the path are illustrated as numbered black spheres. The anion in its binding site is a green sphere. Helices and residues at the interface between subunits A and B are labeled. **a**: view within a membrane slab. **b**: view from the cytoplasm.